Direct laser patterning of ruthenium below the optical diffraction limit

Lorenzo Cruciani ✉ (ID) ; Marnix Vreugdenhil (ID) ; Stefan van Vliet (ID) ; Ester Abram (ID) ; Dries van Oosten (ID) ; Roland Bliem (ID) ; Klaasjan van Druten (ID) ; Paul Planken (ID)

Check for updates

View Online

Export Citation

23 April 2024 07:51:37

Direct laser patterning of ruthenium below the optical diffraction limit

Lorenzo Cruciani,[1,2,a)] (iD) Marnix Vreugdenhil,[3] (iD) Stefan van Vliet,[1] (iD) Ester Abram,[1,2] (iD) Dries van Oosten,[3] (iD)
Roland Bliem,[1,2] (iD) Klaasjan van Druten,[2] (iD) and Paul Planken[1,2] (iD)

AFFILIATIONS

[1]Advanced Research Center for Nanolithography, Science Park 106, 1098 XG Amsterdam, The Netherlands
[2]Van der Waals-Zeeman Institute, Institute of Physics, University of Amsterdam, Science Park 904, 1098 XH Amsterdam, The Netherlands
[3]Debye Institute for Nanomaterials Science and Center for Extreme Matter and Emergent Phenomena, Utrecht University, Princetonplein 5, 3584 CC Utrecht, The Netherlands

[a)]Author to whom correspondence should be addressed: cruciani@arcnl.nl

ABSTRACT

We describe a method that can be used to produce ruthenium/ruthenium oxide patterns starting from a ruthenium thin film. The method is based on highly localized oxidation of a small surface area of a ruthenium film by means of exposure to a pulsed laser under ambient conditions. Laser exposure is followed by dissolution of the un-exposed ruthenium in a NaClO solution, which leaves the conductive, partially oxidized ruthenium area on the substrate. Spatially selective oxidation, material removal, and, by implication, patterning, are, therefore, achieved without the need for a photoresist layer. Varying the exposure laser parameters, such as fluence, focus diameter, and repetition rate, allows us to optimize the process. In particular, it enables us to obtain circular Ru/RuO$_2$ islands with a sub-diffraction-limited diameter of about 500 nm, for laser exposure times as short as 50 ms. The capability to obtain such small islands suggests that heat-diffusion is not a limiting factor to pattern Ru by laser heating on a (sub-)micron scale. In fact, heat diffusion helps in that it limits the area where a sufficiently high temperature is reached and maintained for a sufficiently long time for oxidation to occur. Our method provides an easy way to produce metallic Ru/RuO$_2$ (sub-)micron structures and has possible applications in semiconductor manufacturing.

In recent years, ruthenium (Ru) has appeared as a promising candidate to replace more conventionally used metals, such as Cu and W in semiconductor device manufacturing.[1–3] A prerequisite for many applications in this field is the capability to produce patterned Ru structures on (sub-)micrometer scales. In optical lithography, structures are usually created by first applying patterned illumination of a photoresist layer deposited onto a substrate. Subsequent removal of the exposed regions of the resist, followed by material deposition, etching, and other steps, is needed to create the pattern.[4] Other methods to fabricate patterns are e-beam lithography,[5] electron beam induced deposition,[6] selective area atomic layer deposition,[7,8] or rheology printing.[9]

Here, we show how direct laser writing can be used to pattern Ru without the need for a photoresist. In our method, ultrashort laser pulses are focused to a small spot on a Ru thin film under ambient conditions. Partial absorption of the light by the Ru increases the local temperature and locally oxidizes the surface of the film. Subsequent etching of the layer using a NaClO solution removes the Ru except in the areas where the surface of the layer has been (partially) oxidized. We find that after exposure times as short as 50 ms, we can fabricate Ru/RuO$_2$ islands with diameters as small as 500 nm. This is three to four times smaller than the focal diameter of the laser beam and, in fact, below the diffraction limit of the optical system. From an application perspective, this capability is particularly interesting for the semiconductor manufacturing industry. Creating these structures requires that the local thermal energy at the Ru surface is larger than the threshold energy needed for oxidation for a sufficiently long time. By adjusting the laser pulse energy, reaching this threshold energy can be limited to the most central part of the Gaussian spatial beam profile, thus creating oxidized areas significantly smaller than the full width at half maximum of the focused beam. Our method constitutes a very simple technique for producing Ru/RuO$_2$ structures with sub-diffraction limited features.

We deposited the ruthenium thin films by magnetron sputtering at an argon plasma pressure of 2×10^{-3} mbar. Both glass and silicon were used as substrates. The substrates were chemically cleaned using a solution of ammonium hydroxide (NH_4OH) with hydrogen peroxide in water and, after that, rinsed in isopropanol.

The calculated penetration depth of light for ruthenium on glass as well as absorbed and reflected fractions of 800 and 1030 nm light are provided in Appendix A.

The Ru/RuO$_2$ islands were fabricated by first exposing the ruthenium samples to laser light. Subsequently, the samples were immersed in a 3%–7% NaClO solution in water. This step causes the un-exposed ruthenium to dissolve, leaving the areas partially oxidized by the laser on the substrate. After that, the samples were first rinsed in demineralized water and subsequently in isopropanol to facilitate the drying.

Figure 1(a) is a scanning electron microscopy (SEM) image of a Ru/RuO$_2$ island obtained by exposing a 50 nm thick Ru-on-silicon sample to a 70 fs, 800 nm wavelength 5.2 MHz repetition rate laser for 15 s, focused to a diameter of about 8 μm. The sample was then rinsed in the NaClO solution for 720 s. We found that a minimum rinse time is required to remove the Ru layer and that longer times are necessary for thicker films. However, once the un-exposed layer is dissolved, rinsing for times up to several hours does not have a significant influence on the island. The island shown in Fig. 1(a) has an approximately round shape and a small diameter of approximately 9 μm.

In Fig. 1(b), we show a photograph of a set of large Ru/RuO$_2$ islands obtained with a weakly focused laser beam. The islands have a shiny metallic look and the surrounding area of the glass substrate appears clean.

We chemically characterized the islands by performing x-ray photoelectron spectroscopy (XPS). This was done on a large island obtained from an 8 nm thick Ru sample on glass, exposed to the laser and rinsed in NaClO. The results (Appendix B, Fig. S1) show that our method produces a partially oxidized Ru film, similar to the one we described previously.[10] This film is a partially oxidized Ru layer in which the oxide is in the rutile phase. By extracting the average oxide thickness from the XPS measurements using the flat overlayer approximation,[11] we found that oxide thicknesses as low as 2.4 nm are already sufficient to prevent the laser-exposed area from being removed by the NaClO solution. If the same measured XPS intensities are used within the hypothetical high-roughness limit of Ru/RuO$_2$ core-shell particles[12] assembled into a layer, this number decreases to 1.4 nm. It is

possible that even thinner rutile-phase RuO$_2$ layers may prevent etching of the Ru in the NaClO solution, but this has not been tested

To gain information on the island-formation process and to find the optimal exposure parameters to create the smallest spots, Ru layers with thicknesses of 8 and 20 nm on a glass substrate were exposed to the same 5.2 MHz-repetition rate laser at different fluences. Throughout this paper, fluence is defined as the single-pulse energy divided by the FWHM area of the laser spot, although exposure is performed with multiple pulses. After exposure, the samples were rinsed with the NaClO solution for 90 s (8 nm) and 210 s (20 nm).

Optical microscopy images of two islands obtained on these samples after exposure to a 9.5 mJ/cm^2 fluence are shown in Fig. 2(a). The observed diameter is approximately 16 μm for the 8 nm film and 13 μm for the 20 nm film. The island obtained from the 8 nm film does not have sharply defined edges. This is also the case for the islands obtained with higher exposure fluences, which results in larger error bars for the areas extracted from this sample.

To learn more about the process resulting in the formation of Ru/RuO$_2$ islands, we performed a Liu analysis.[13] This analysis is valid for laser-induced processes occurring at fluences exceeding a certain threshold and when the laser beam profile is Gaussian. Often, in these cases, the area of a laser-induced material modification scales linearly with the natural logarithm of the fluence. When these conditions are satisfied, it is possible to extract the threshold fluence at which the islands are formed by extracting the fluence level where the island area is zero from a linear fit to the data.

The Liu plots, obtained from optical microscopy images similar to the ones shown in Fig. 2(a), are shown in Fig. 2(b). For both the 8 nm and the 20 nm thick films, the figure clearly shows that the area of the islands does not scale linearly with the logarithm of the exposure fluence. The vertical lines in the plot indicate the fluence beyond which optical microscopy images show a darker region in the center of the island. This was identified as an ablated region. The lines are located at a fluence of 17 mJ/cm^2 for the 8 nm thick film and 23 mJ/cm^2 for the 20 nm thick film. We note that melting can already occur at fluence levels somewhat below the damage threshold. The effect of melting on the formation of the oxide is at present unknown. Understanding the effect of ruthenium melting on the island formation process is an interesting question. However, given the high melting temperature of ruthenium (2603 K), it might not be as relevant from an application point of view as it increases the risk of damaging the material underneath the ruthenium and is, therefore, beyond the scope of this paper. Fluences below the range reported in Fig. 2(a) were also tested, but no islands were observed. This applies also to the other Liu plots presented in this work.

Since the spots obtained for thicker films produced more uniform and smaller islands, we also tested our method on 50-nm-thick Ru samples for two different exposure times: 5 and 15 s. After exposure, the samples were rinsed in the NaClO solution for 390 s. Note that the thickness of 50 nm was chosen more or less randomly and, for applications in the semiconductor manufacturing industry, it would also be interesting to test our method with even thicker films, up to 100 nm, although we expect to obtain similar results.

Selected microscopy images of islands are shown in Fig. 2(c) for both exposure times. These islands were obtained with an exposure fluence of 9.5 mJ/cm^2. Their diameters are 7 μm (5 s exposure) and 9 μm (15 s exposure), close to the illumination spot size ($\sim$ 8 μm).
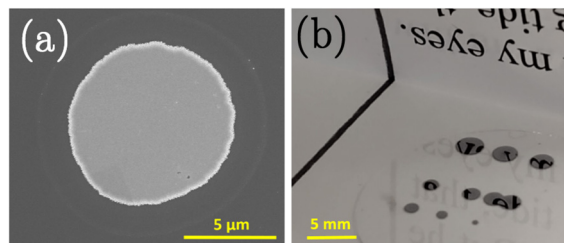

FIG. 1. (a) SEM image of an island obtained with the 5.2 MHz repetition rate laser focused to a spot with a diameter of about 8 μm. This island has a diameter of approximately 9 μm. (b) Photograph of a set of Ru islands on a glass substrate, placed on a piece of paper with a rectangular fold, illustrating the high optical reflectivity of the islands.
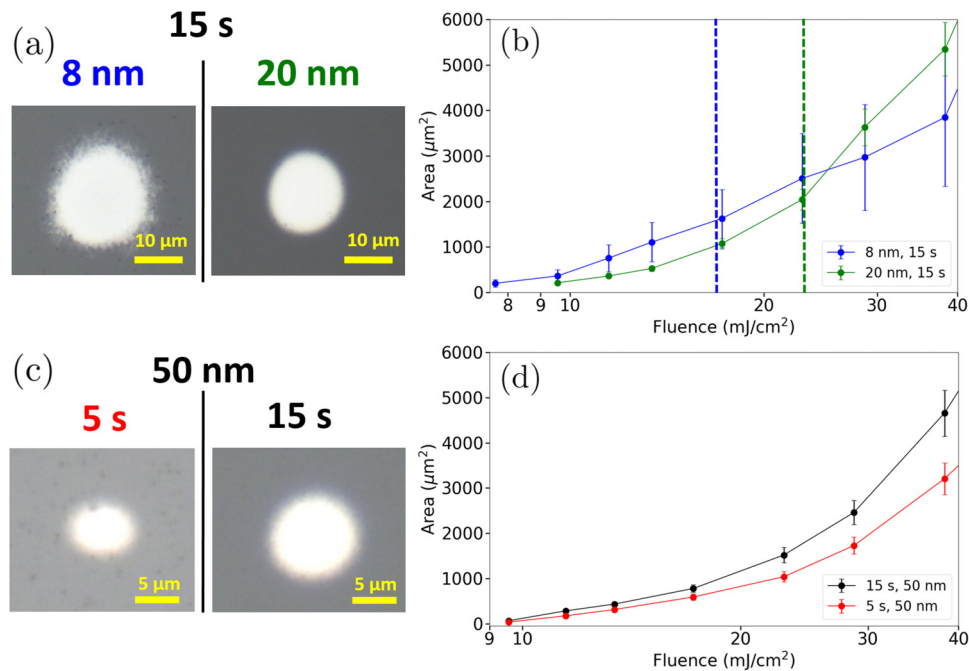
FIG. 2. (a) Optical microscopy images of the islands relative to the Liu plot in the sub-figure (b). (b) Liu plot of the RuO$_2$/Ru islands obtained after 15 s exposure of 8 (blue) and 20 nm (green) Ru films on glass to the high repetition rate, 800 nm laser. The dashed vertical lines correspond to the measured ablation thresholds. (c) Optical microscopy images of the islands relative to the Liu plot in the sub-figure (d). (d) Liu plot obtained from a 50 nm Ru film on glass exposed for 15 s (black) and 5 s (red) to the high repetition rate, 800 nm laser.

The Liu plots obtained for the 5 s (red) and 15 s (black) exposure times are shown in Fig. 2(d). Both curves are similar to the ones obtained for the 8 and 20 nm samples, showing super-linear dependence on the logarithm of the exposure fluence. For each fluence, the red curve indicates that, overall, a 5 s exposure leads to smaller areas than the ones obtained with the 15 s exposure.

The non-linearity of the Liu plots is an indication that in-plane heat transport may affect the island size. Additional evidence of in-plane heat transport is the observation of islands with an area much larger than the laser spot size, at high exposure fluences. Optical microscopy images of such areas, with a diameter of approximately 80 μm (ten times larger than the exposure spot diameter), are shown in Appendix C, Fig. S2.

The above-mentioned fact suggests that varying the number of laser pulses, as well as the time interval between them, has an influence on the formation of the Ru/RuO$_2$ islands. Furthermore, smaller islands could be achievable by tighter focusing. For this reason, we tested our method with a lower repetition rate laser capable of generating a variable number of pulses. The laser delivers 200 fs pulses at a 1030 nm central wavelength with a repetition rate of 200 kHz. This source was focused onto the sample to spots with a diameter of approximately 2 μm. This system is described in more detail elsewhere.[14]

Figure 3(a) is an optical microscopy image of a typical grid of islands obtained using the aforementioned illumination system on a 50 nm Ru film on glass. Each spot was exposed to different numbers of laser pulses at a (single-pulse) fluence of 18.2 mJ/cm^2. The number of pulses increases in a "meandering" fashion from the top-right corner of the image to the bottom-right one and is varied from 1 to 50 000.

The islands are remarkably small: most of them have sub-micrometer diameters and none of them exceeds the illumination spot size by more than a few percent.

The size of one the smallest islands that we could obtain with the low repetition rate laser is estimated by performing SEM. In addition,
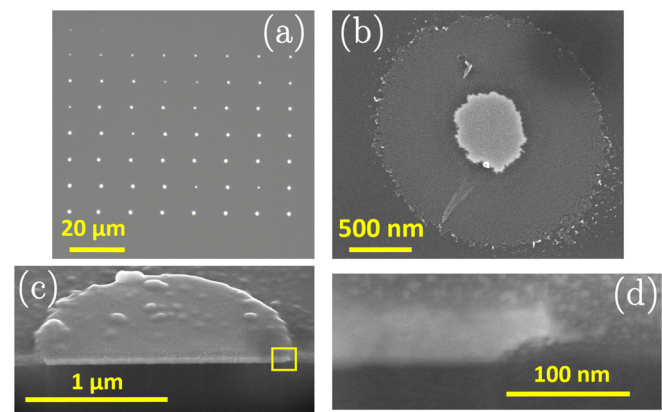
FIG. 3. (a) Optical microscopy image of a grid of Ru/RuO$_2$ islands on silicon obtained with a 2 μm beam diameter of the 200 kHz repetition rate, 1030 nm laser. (b) SEM image of a typical island. (c) Cross-sectional SEM of an island viewed at an angle of 52°. (d) Detail of the region highlighted by the yellow square in image (c), showing that the amount of under-etching is limited to a distance of ~35 nm from the edge of the island.

this allows us to characterize the island morphology. As SEM on glass is complicated by charge accumulation, we fabricated islands on a 50 nm Ru film on silicon, for which charging is not an issue.

A typical SEM image of one of the smallest islands that we obtained is shown in Fig. 3(b). The central Ru/RuO_2 region has an exceptionally small diameter of approximately 500 nm, four times smaller than the diffraction limit of the objective used to focus the laser. The central area is surrounded by an additional region having a different appearance and approximately the same diameter as the illumination beam.

In an attempt to identify the content of the region surrounding the central island, we performed energy-dispersive x-ray spectroscopy (EDX).[15] The results, presented in Appendix D, Figs. S3 and S4, show the presence of Ru but no other potential contaminants, such as sodium or chlorine. We note that this region is not affected by additional rinsing in the NaClO solution or by varying the NaClO concentration between 2% and 5% and 6%–14%.

To learn more about a typical Ru/RuO_2 island morphology and to determine the amount of under-etching, we performed cross-sectional SEM imaging on an island obtained from a 50 nm thick Ru film on Si, exposed to the 200 kHz laser focused to a 2 μm spot size. This was done by first depositing a layer of platinum over the island and by subsequently removing a section of the island with a focused ion beam (FIB). The Pt layer facilitates the attainment of sharp edges in the FIB cut. The resulting image, recorded by orienting the sample at an angle of 52° with respect to the detector, is shown in Fig. 3(c). The island has a ~2 μm diameter and a flat cross section. Figure 3(d) is the high magnification image of the area inside the yellow square in Fig. 3(c). Here, it can be seen that the under-etching is limited to a distance from the edge of ~35 nm.

Liu plots of the islands obtained by exposing 50-nm-thick Ru films on glass to different numbers of laser pulses from the 200 kHz repetition rate laser are shown in Fig. 4(a). The areas of the islands were extracted from optical microscopy images similar to the one shown in Fig. 3(a). Since the island size, in this case, is close to the resolution limit of the optical microscope, the resulting areas have a large error bar. Unlike the case of exposure to the 5.2 MHz repetition rate laser (Fig. 2), the areas now depend approximately linearly on the logarithm of the exposure fluence. Furthermore, at a given fluence, the island area increases with an increasing number of pulses. In this case, the fluence range was fine tuned in order to include fluences high enough for island formation for many different numbers of pulses, while keeping the fluence below the ablation threshold. This results in a narrow fluence interval. The linearity of the Liu plots over a broader fluence range is confirmed in Appendix E, Fig. S5.

The effect of exposure to different numbers of pulses is further examined by performing a linear fit on a large set of Liu plots, similar to those of Fig. 4(a) and by extracting the intercepts with the x axis. This value corresponds to the (single-pulse) oxidation threshold-fluence F_0, which is then plotted as a function of the number of pulses in Fig. 4(b). This shows a modest linear decrease in F_0 from a value of 17.5 ± 0.5 mJ/cm^2 for approximately 7000 pulses, down to a value of 16.1 ± 0.5 mJ/cm^2 for 16 000 pulses. From here, it keeps decreasing, although with a lower slope. The cumulative effect of exposure to multiple laser pulses, therefore, becomes less important for $N \gtrsim 16\,000$. We note that 10 000 pulses corresponds to a total exposure time of 50 ms.
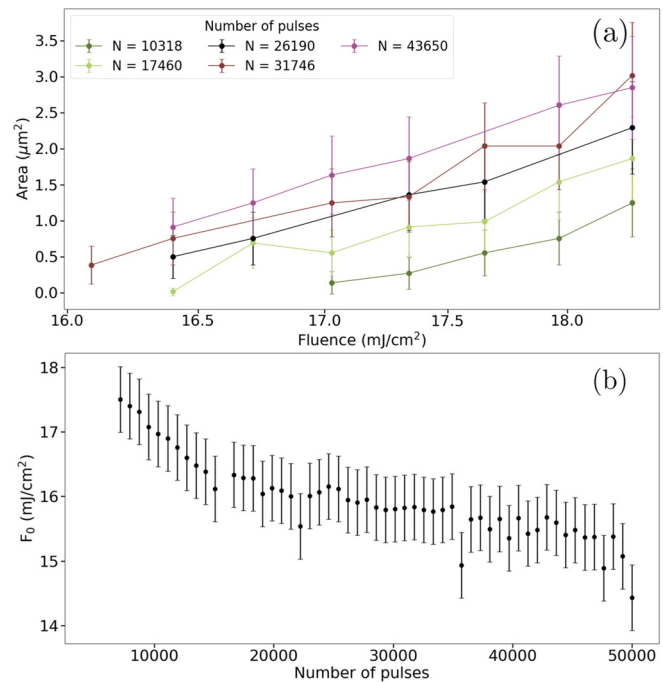

FIG. 4. (a) Liu plot obtained from a 50 nm Ru film on glass exposed to the 200 kHz repetition rate laser for different numbers of laser pulses. (b) Threshold fluences for islands formation (F_0) as a function of the number of pulses. This quantity is obtained from the intercepts with zero from the Liu plots similar to the one in (a).

To confirm that our process produces electrically conductive samples, we measured the sheet resistance of an oxidized sample rinsed in the NaClO solution, using the four-point probe van der Pauw method[16] and compared it with an as-deposited Ru sample, which has a sheet resistance of 4.3 Ω/sq. Oxidation was performed in an oven, in order to oxidize the whole sample, which is necessary for the four-point probe measurement, at 350 °C at a 10^{-4} mbar O_2 atmosphere for 75 min. The sample was then rinsed in the NaClO solution for 390 s. In this case, we obtained a sheet resistance of 8.6 Ω/sq.: only a twofold increase with respect to the pristine Ru sample. This result shows that partial oxidation and subsequent immersion in the NaClO solution do not cause a dramatic increase in resistivity and produce conductive samples.

For both high- and low-repetition rate lasers, we observed the effect of multiple-pulse exposure: with the 5.2 MHz repetition rate, we found non-linear Liu plots and islands with an area largely exceeding the illumination spot size; with the 200 kHz repetition rate laser, we observed a dependence of the oxidation threshold fluence on the number of laser pulses. All of these effects could either be due to a (high) temperature increase resulting from multiple pulse heat accumulation in combination with in-plane heat transport, by an accumulation of (single-pulse) oxidation steps, or by a combination of the two.

Heat accumulation is most likely to occur with the 5.2 MHz repetition rate system due to the short time interval between the pulses (192 ns) and the relatively long exposure times (5–15 s). In this case, after each laser pulse, the illuminated area does not return to room temperature before the arrival of the next one. This results in a high

temperature increase which, together with in-plane heat transport, produces a super-linear growth of the (partially) oxidized area as a function of the logarithm of single-pulse exposure fluence, as observed in Fig. 2.

The aforementioned mechanism is less likely to apply to the case of the 200 kHz repetition rate laser. In this case, the Liu plots are approximately linear [Fig. 4(a)], and the island area does not exceed the exposure area as dramatically. The accumulation effect manifests itself as an increase in the island area at a fixed exposure fluence, for an increasingly higher number of pulses, as well as a modest decrease in the threshold fluence F_0 [Fig. 4(b)]. We attribute these features to accumulation of oxidation: each laser pulse oxidizes a fraction of the thickness of the illuminated area. The minimum fluence necessary to oxidize a thick enough layer to prevent dissolution in NaClO, therefore, depends on the number of laser pulses. This process results in a linear dependence of the island area on the logarithm of the exposure fluence as in-plane heat transport does not seem to increase the island size dramatically.

In conclusion, we have demonstrated a method for producing conductive Ru/RuO$_2$ islands. We obtained islands with a diameter as small as 500 nm using a 2 μm beam diameter at a wavelength of 1030 nm. Our method can produce sub-diffraction limited island sizes, which is somewhat surprising for a thermally driven process. We note that, in principle, once the sub-diffraction-limited Ru/RuO$_2$ patterns are obtained, the RuO$_2$ can be reduced back to Ru by exposure to reducing agents, such as hydrogen gas at high temperatures.[17,18] Smaller features may be obtained by further fine tuning parameters, such as laser wavelength, beam size, and exposure time. Finally, we note that laser-induced oxidation should be taken into account in the interpretation of pump-probe measurements on Ru[10,19,20] and, possibly, on other metals as well.[21] Our measurements shed some light on the circumstances under which this can occur.

See the supplementary material for the details regarding penetration depth and fraction of absorbed and reflected light for ruthenium on glass; x-ray photoelectron spectroscopy measurements; optical microscopy images of islands largely exceeding the illumination diameter; energy-dispersive x-ray spectroscopy measurements; and Liu-plot over an extended fluence range.

AUTHOR DECLARATIONS
Conflict of Interest

The authors have no conflicts to disclose.

Author Contributions

Lorenzo Cruciani: Conceptualization (equal); Data curation (lead); Formal analysis (lead); Investigation (equal); Methodology (equal); Visualization (equal); Writing – original draft (equal); Writing – review & editing (equal). **Marnix Vreugdenhil:** Investigation (supporting); Writing – review & editing (supporting). **Stefan Van Vliet:** Conceptualization (supporting); Investigation (supporting); Writing – review & editing (equal). **Ester Abram:** Investigation (supporting); Writing – review & editing (equal). **Dries van Oosten:** Writing – review & editing (equal). **Roland Bliem:** Writing – review & editing (equal). **Klaasjan van Druten:** Conceptualization (equal); Formal analysis (equal); Funding acquisition (equal); Methodology (equal); Project administration (equal); Supervision (equal); Writing – review & editing (equal). **Paul Planken:** Conceptualization (equal); Formal analysis (equal); Funding acquisition (equal); Methodology (equal); Project administration (equal); Supervision (equal); Validation (equal); Writing – review & editing (equal).

DATA AVAILABILITY

The data supporting the findings of this study are available from the corresponding author upon reasonable request.

REFERENCES

[1]E. Milosevic, S. Kerdsongpanya, A. Zangiabadi, K. Barmak, K. R. Coffey, and D. Gall, "Resistivity size effect in epitaxial Ru(0001) layers," J. Appl. Phys. **124**, 165105 (2018).

[2]H. Zhong, G. Heuss, and V. Misra, "Electrical properties of RuO$_2$ gate electrodes for dual metal gate Si-CMOS," IEEE Electron Device Lett. **21**, 593–595 (2000).

[3]I.-H. Kim and K.-B. Kim, "Ruthenium oxide thin film electrodes for supercapacitors," Electrochem. Solid-State Lett. **4**, A62 (2001).

[4]T. Ito and S. Okazaki, "Pushing the limits of lithography," Nature **406**, 1027–1031 (2000).

[5]M. Altissimo, "E-beam lithography for micro-/nanofabrication," Biomicrofluidics **4**, 026503 (2010).

[6]W. F. van Dorp and C. W. Hagen, "A critical literature review of focused electron beam induced deposition," J. Appl. Phys. **104**, 081301 (2008).

[7]S. M. George, "Atomic layer deposition: An overview," Chem. Rev. **110**, 111–131 (2010).

[8]A. J. M. Mackus, M. J. M. Merkx, and W. M. M. Kessels, "From the bottom-up: Toward area-selective atomic layer deposition with high selectivity," Chem. Mater. **31**, 2–12 (2019).

[9]T. Kaneda, D. Hirose, T. Miyasako, P. T. Tue, Y. Murakami, S. Kohara, J. Li, T. Mitani, E. Tokumitsu, and T. Shimoda, "Rheology printing for metal-oxide patterns and devices," J. Mater. Chem. C **2**, 40–49 (2014).

[10]L. Cruciani, S. van Vliet, A. Troglia, R. Bliem, K. van Druten, and P. Planken, "Femtosecond laser-induced emission of coherent terahertz pulses from ruthenium thin films," J. Phys. Chem. C **127**, 22662–22672 (2023).

[11]A. Jablonski and J. Zemek, "Overlayer thickness determination by XPS using the multiline approach," Surf. Interface Anal. **41**, 193–204 (2009).

[12]A. G. Shard, "A straightforward method for interpreting XPS data from core–shell nanoparticles," J. Phys. Chem. C **116**, 16806–16813 (2012).

[13]J. M. Liu, "Simple technique for measurements of pulsed Gaussian-beam spot sizes," Opt. Lett. **7**, 196–198 (1982).

[14]M. Vreugdenhil and D. van Oosten, "A highly automated apparatus for ultra-fast laser ablation studies," Rev. Sci. Instrum. **93**, 073003 (2022).

[15]A. Z. D. R. Irene Prencipe, D. Dellasega, and M. Passoni, "Energy dispersive x-ray spectroscopy for nanostructured thin film density evaluation," Sci. Technol. Adv. Mater. **16**, 025007 (2015).

[16]F. Oliveira, R. Cipriano, F. Silva, E. Romão, and C. dos Santos, "Simple analytical method for determining electrical resistivity and sheet resistance using the van der Pauw procedure," Sci. Rep. **10**, 16379 (2020).

[17]D. Ugur, A. J. Storm, R. Verberk, J. C. Brouwer, and W. G. Sloof, "Kinetics of reduction of a RuO_2(110) film on Ru(0001) by H_2," J. Phys. Chem. C **116**, 26822–26828 (2012).

[18]A. Izumi, T. Ueno, Y. Miyazaki, H. Oizumi, and I. Nishiyama, "Reduction of oxide layer on various metal surfaces by atomic hydrogen treatment," Thin Solid Films **516**, 853–855 (2008).

[19]H. J. Shin, J.-M. Lee, S. Bae, W.-H. Kim, and S. Sim, "Metal-insulator transition and interfacial thermal transport in atomic layer deposited Ru nanofilms characterized by ultrafast terahertz spectroscopy," Appl. Surf. Sci. **563**, 150184 (2021).

[20]F. Akhmetov, I. Milov, S. Semin, F. Formisano, N. Medvedev, J. M. Sturm, V. V. Zhakhovsky, I. A. Makhotkin, A. Kimel, and M. Ackermann, "Laser-induced electron dynamics and surface modification in ruthenium thin films," Vacuum **212**, 112045 (2023).

[21]J. Hohlfeld, S.-S. Wellershoff, J. Güdde, U. Conrad, V. Jähnke, and E. Matthias, "Electron and lattice dynamics following optical excitation of metals," Chem. Phys. **251**, 237–258 (2000).

23 April 2024 07:51:37